Optical control of an atomic inner-shell x-ray laser

Gábor Darvasi,[1] Christoph H. Keitel,[1] and Christian Buth[1,2,*]
[1]*Max-Planck-Institut für Kernphysik, Saupfercheckweg 1, 69117 Heidelberg, Germany*
[2]*Argonne National Laboratory, Argonne, Illinois 60439, USA*
(Received 23 April 2012; published 21 January 2014)

X-ray free-electron lasers have had an enormous impact on x-ray science by achieving femtosecond pulses with unprecedented intensities. However, present-day facilities operating by the self-amplified spontaneous emission principle have a number of shortcomings; namely, their radiation has a chaotic pulse profile and short coherence times. We put forward a scheme for a neon-based atomic inner-shell x-ray laser (XRL) which produces temporally and spatially coherent subfemtosecond pulses that are controlled by and synchronized to an optical laser with femtosecond precision. We envision that such an XRL will allow for numerous applications such as nuclear quantum optics and the study of ultrafast quantum dynamics of atoms, molecules, and condensed matter.

DOI: 10.1103/PhysRevA.89.013823 PACS number(s): 42.55.Vc, 32.80.Aa, 41.60.Cr, 42.50.Hz

I. INTRODUCTION

An x-ray laser (XRL) is an old goal of laser physics [1,2]. Extending the superior coherence, intensity, and controlled pulse properties of lasers to the x-ray regime has the potential to revolutionize x-ray science by bringing unprecedented intensities, temporal and spatial control of beam properties, and ultrashort pulses to the x-ray scientist. Such an XRL would be suitable for numerous applications from ionic and nuclear quantum optics [3] to high-energy physics and astrophysics [4] and it offers perspectives for the measurement and control of quantum dynamics of matter on an ultrafast time scale [5]. X-ray free-electron lasers (FELs) [6] such as the Linac Coherent Light Source (LCLS) [7] have reached several of the goals laid out for XRLs, namely, ultraintense, tunable, femtosecond x-ray pulses. However, present-day x-ray FELs, operating by the principle of self-amplified spontaneous emission (SASE) [7,8], suffer from a number of shortcomings compared with optical lasers. Specifically, they lack controllability of the pulse properties, spectral narrowness, and photon energy stability [7]. Furthermore, there is a jitter between FEL x rays and an optical laser which can only be determined with the precision of several tens of femtoseconds [9]. Yet there are exciting novel facilities such as FERMI@Elettra [10] and self-seeding at LCLS for hard x rays [11] becoming available that use seeding to improve on the properties of the x-ray pulses, reducing their bandwidth and the fluctuations of the pulse shapes.

Lasing schemes from the optical regime cannot be transferred simply to the x-ray regime due to the unfavorable scaling of the cross section for stimulated emission [1], the lack of high-reflectivity mirrors for x rays [2], and the short duration of population inversion caused by inner-shell hole decay [12,13]. Lasing in the xuv and soft x-ray regimes has been accomplished with plasma-based XRLs via collisional or recombinational pumping [2]. However, these techniques have not yet reached beyond the water window starting at 276.2 eV.

A scheme for x-ray lasing in the keV regime was proposed by Duguay and Rentzepis in 1967 based on x-ray emission from inner-shell transitions in core-ionized atoms [14] which may be produced by focusing an intense x-ray beam from a FEL into a gas cell with atoms [15,16]. Here one exploits that, at a given photon energy above but close to an inner-shell edge, these tightly bound inner-shell electrons are much more likely to interact with FEL x rays than electrons in other shells [12], and thus an inner-shell vacancy is produced leaving the cation in a state of population inversion with respect to radiative transitions of electrons from higher-lying shells into the vacancy. X-ray lasing may occur in a macroscopic medium of such cations, in analogy to optical lasers, by the propagation of initially spontaneously emitted x rays through the medium leading to stimulated emission of x rays.

In this work, we would like to present the optical control of a modified Duguay and Rentzepis scheme for an atomic inner-shell XRL. The x-ray lasing scheme is presented in Sec. II, the small-signal gain (SSG) and its dependence on the optical laser intensity are discussed in Sec. III, and the propagation of the FEL x rays, the optical laser, and the XRL light are examined in Sec. IV. Finally, conclusions are drawn in Sec. V. Atomic units [17] are used throughout unless stated otherwise.

II. X-RAY LASING SCHEME

We develop a modified Duguay-Rentzepis scheme [14] for which atoms are core excited instead of core ionized by FEL x rays. The principle is illustrated in Fig. 1 by which x-ray lasing proceeds as follows [18]: first, atoms are core excited by FEL x-ray absorption producing a state of population inversion [Fig. 1(a)]. Second, photons are emitted through spontaneous radiative decay of some of the core-excited atoms [Fig. 1(b)]. Third, a fraction of these photons copropagates with the FEL pulse through the medium and induces stimulated x-ray emission from other core-excited ions farther downstream in straight conceptual analogy to optical lasers [1]. Due to longitudinal pumping, x-ray lasing only occurs in the propagation direction of the pump pulse [16,18]. Until recently it was not possible to realize such an XRL due to the high pump x-ray intensity [19] that is necessary to excite the lasing medium faster than inner-shell holes decay [12,13].

*Corresponding author. Present address: Max-Planck-Institut für Quantenoptik, Hans-Kopfermann-Straße 1, 85748 Garching bei München, Germany. Electronic address: christian.buth@web.de

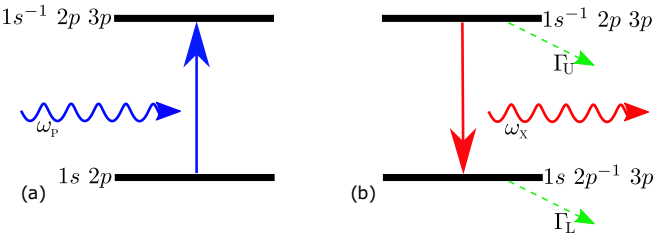

FIG. 1. (Color online) Schematic of x-ray lasing in core-excited neon with pumping by an x-ray FEL. (a) Neon atoms are excited by x rays from a FEL from the ground state to the $1s^{-1}\,2p3p$ core-excited state. (b) X-ray lasing occurs on the $1s^{-1}\,2p\,3p \rightarrow 1s\,2p^{-1}\,3p$ transition. Furthermore, Γ_U and Γ_L are the decay widths of the upper and lower lasing states, respectively.

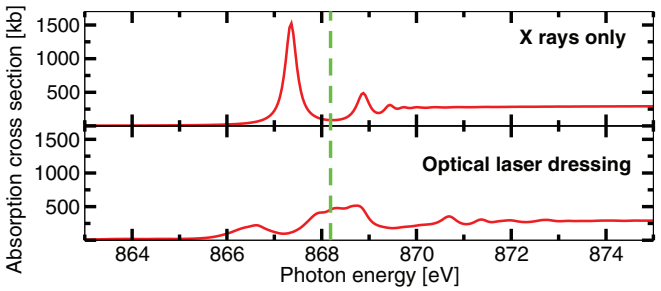

FIG. 2. (Color online) X-ray absorption cross section by core electrons of neon near the K edge for the field-free case (top) and for optical laser dressing at 10^{13} W/cm^2 (bottom) with an 800 nm laser. The x rays and the optical light are linearly polarized and have parallel polarization vectors. The dashed green line indicates the central FEL photon energy at $\omega_P = 868.2$ eV. Adapted from Ref. [22].

The advent of xuv and x-ray FELs has reinvigorated interest in Duguay-Rentzepis-style schemes, producing a number of theoretical studies [15,16,18] and the experimental realization for neon in 2011 at LCLS [20]. Although this simple, uncontrolled XRL scheme produces pulses with a single, fully coherent intensity spike, it still suffers from a number of shortcomings: the pulse properties depend on the temporal shape of the pump pulse and multicolor lasing may occur [16] for suitably high FEL x-ray photon energies due to x-ray lasing on transitions in highly charged ions. Multiple uncontrolled pulses may lead to complications in experiments harnessing the XRL light. However, multicolor x-ray lasing can be suppressed in the Duguay-Rentzepis scheme with core ionization [14], if the photon energy of the FEL x rays is tuned only slightly above the inner-shell absorption edge. Then the FEL photon energy is not high enough to coreionize cations; yet core excitations of cations are energetically accessible, thus leading to more than one XRL transition [21]. Although multicolor x-ray lasing was predicted [16], it has not been observed experimentally yet [20].

We put forward an XRL scheme for neon that is controlled by optical light. The FEL x-ray photon energy, $\omega_P = 868.2$ eV, is tuned below the K edge slightly above the $1s \rightarrow 1s^{-1}3p$ resonance (Fig. 1), as indicated by the dashed (green) line in the x-ray absorption cross section by core electrons of neon in Fig. 2. We choose a FEL x-ray photon energy of ω_P also for the FEL x-ray-only case in order to facilitate comparison of the FEL x-ray-only case with the optically controlled XRL case. Namely, for this choice of ω_P, the FEL x-ray-only case represents the optical-laser-off limit of the optically controlled XRL which allows the strong increase of the small-signal gain with the optical laser intensity as shown in Fig. 3 and discussed in Sec. III. Hence, only in this case, strong optical control of the XRL is exerted. For the FEL x rays only, core excitation is off resonant and thus fairly inefficient (Fig. 2, top), if the bandwidth of the FEL x rays is limited sufficiently, e.g., by seeding techniques [10,11]. X-ray lasing occurs on the superposition of $1s^{-1}\,2p\,3p \rightarrow 1s\,2p^{-1}\,3p$ and $1s^{-1}\,2p\,4p \rightarrow 1s\,2p^{-1}\,4p$ transitions leading to a two-peak feature around 849 eV for highly monochromatized x rays [21]. We assume a full width at half maximum (FWHM) bandwidth of the FEL x rays of $\Delta\omega_P = 0.4$ eV which is sufficiently broad such that the two-peak structure disappears.

An optical laser with intensity I_L, that copropagates with the FEL x rays, modulates the x-ray absorption cross section by core electrons of neon $\sigma_X(I_L,\omega)$ [22–24], as shown in Fig. 2 (bottom), which thus becomes dependent on I_L. The $\sigma_X(I_L,\omega_P)$ is increased more than sixfold from 86 to 510 kb when I_L is increased from 0 to 10^{13} W/cm^2 for an optical dressing laser with 800 nm wavelength [22]. For this study, the core-excitation cross section $\sigma_X(I_L,\omega)$ is calculated as a function of the x-ray photon energy ω at nine different optical laser intensities I_L with the DREYD program [22–27], whereby the wavelength of the optical laser is not varied [28]. This dependence of $\sigma_X(I_L,\omega_P)$ on I_L permits a high degree of control over the absorption of FEL x rays which determines the probability for an atom to be core excited and thus to enter a state of population inversion (Fig. 1). The Floquet approximation is used to determine $\sigma_X(I_L,\omega)$ for an atom in two-color cw light [26]. As we employ light pulses with a duration of only a few optical cycles, the Floquet method represents an approximation to the non-cw solution for finite-duration light pulses. In Fig. 2 of Ref. [29] results from the solution of the time-dependent Schrödinger equation are compared with Floquet theory for a three-cycle FWHM duration pulse interacting with a hydrogen atom at a photon energy of 54.4 eV. The parameters used to produce that figure and the situation considered here are not identical and thus some moderate quantitative deviations are possible. Further details on ultrashort pulse propagation in a macroscopic medium are examined in Ref. [27] based on the solution of the combined Maxwell and Schrödinger equations.

The optical laser rapidly ionizes Rydberg electrons, e.g., in the neon $3p$ orbital, via multi-optical-photon absorption leading to a large induced width for core-excited states of approximately 0.54 eV [22]. Hence, a mixture of core-excited and core-ionized atoms is found in the gas cell. For core-ionized neon atoms, the x-ray emission spectrum [30] peaks at 848.66 eV which is within the linewidth of the emission from core-excited states [21]. Using a detector with a resolution that is too low to resolve the fluorescence lines of core-excited neon, we need not distinguish between core-excited [21] and core-ionized [30] neon atoms. The lifetime of a core-excited state is only minutely influenced by the presence of a Rydberg electron with respect to the

lifetime of a core-ionized state [31] and is 2.4 fs, implying an XRL linewidth of $\Delta\omega_X = 0.27$ eV [13]. Furthermore, optical laser ionization, Auger decay, and the very short coherence time of SASE FEL x rays cause strong decoherence, making semiclassical laser theory [1] applicable to describe the effect of optical laser dressing on x-ray lasing.

III. SMALL-SIGNAL GAIN

The small-signal gain (SSG) [1,16,18] represents the amplification of spontaneously emitted x rays on the XRL transition in the exponential gain regime:

$$g(t) = \sigma_{se} N_U(t) - \sigma_{ab} N_L(t), \tag{1}$$

where $N_U(t)$ is the upper-level occupancy (or population), $N_L(t)$ is the lower-level occupancy, and σ_{se} and σ_{ab} are the stimulated emission and absorption cross sections, respectively, with

$$\sigma_{se} = A_{U\to L} \frac{2\pi c^2}{\omega_X^2 \Delta\omega_X}, \quad \sigma_{ab} = \sigma_{se} \frac{g_U}{g_L}, \tag{2}$$

where $A_{U\to L} = 5.9 \times 10^{12}$ s^{-1} is the Einstein coefficient for spontaneous emission on the XRL transition, c is the speed of light in vacuum, and $g_U = 6$ and $g_L = 1$ are the probabilistic weights of the upper and lower lasing levels, respectively, in our case. The cross sections in Eq. (2) have been evaluated at the peak of the line, assuming a Lorentzian line shape [16,18]. The SSG in Fig. 3(b) is calculated with Eqs. (1) and (2) for a single atom determining the level populations with rate equations similar to Eqs. (3), (6), and (7) below, however, without the dependence on the z coordinate and the influence of the XRL light on the level populations. We generate SASE FEL x rays by the partial-coherence method [32] using a Gaussian spectrum centered at ω_P with a FWHM of $\Delta\omega_P = 0.4$ eV. The FEL beam is assumed to be Gaussian with a waist of $w_0 = 10$ μm [7]. We place the neon atoms in a gas cell around the beam waist with a length of $L = 5$ mm.

In Fig. 3(a), we show optical laser pulses [33] at three different positions with respect to a single FEL x-ray pulse; in Fig. 3(b), we display the SSG for pumping with this FEL pulse with and without optical laser dressing for each of the three positions. A pronounced modulation of the SSG occurs only for the dashed red optical laser pulse. The SSG is modified substantially only if the optical laser pulse overlaps with the rising flank of the FEL pulse. Otherwise, the K-shell absorption cross section is modified either too early—before the x rays from the FEL interact with the atoms—or too late, after a substantial fraction of the atoms has already been destroyed, i.e., excited or ionized.

Because the shape of the x-ray pulse from a SASE FEL varies on a shot-to-shot basis [7,8], we present SSG results averaged over 500 single-shot calculations in Fig. 3(b) for the three positions of the optical dressing laser. The average SASE FEL pulse over 500 shots is shown in Fig. 3(a). The importance of the relative timing between the FEL pulse and the optical laser pulse is also reflected in the averaged calculations. The average SSG increases from $0.16\,a_0^2$ to $0.4\,a_0^2$ for the optical laser pulse drawn as a dashed red line in Fig. 3(a) while no substantial increase of the SSG is observed for the dashed blue and dashed green positions of the optical laser pulse. It

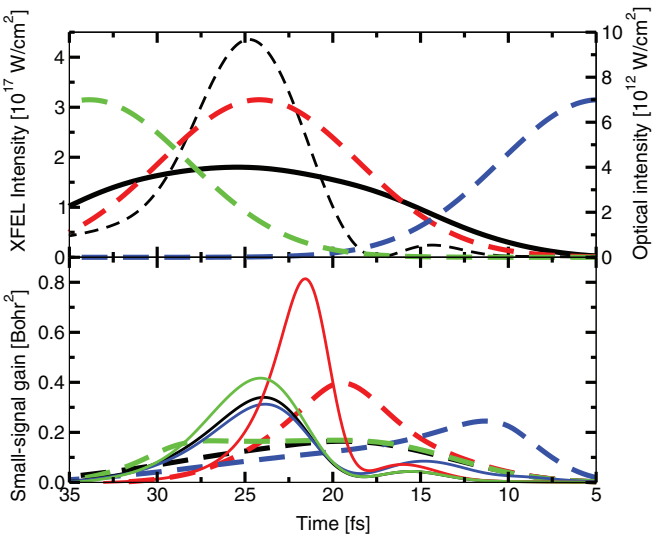

FIG. 3. (Color) (a) The dashed black line is the amplitude of a single SASE FEL x-ray pulse. The dashed red, blue, and green lines are five-optical-cycle (13 fs) FWHM duration pulses of the optical dressing laser at three different positions with respect to the FEL x-ray pulse. The solid black line is the average over 500 SASE FEL pulses. We assume 3×10^{13} x rays in, on average, 21.5 fs FWHM long pulses, focused to a 10 μm spot at a bandwidth of 0.4 eV. (b) The solid black line shows the single-shot SSG in the field-free case if the XRL is pumped with the dashed black SASE FEL pulse from (a) which has a FWHM duration of 7.3 fs; the solid red, blue, and green lines show the single-shot SSG for laser dressing with the optical laser pulse of matching color from (a). The average of the SSG over 500 SASE FEL pulses for the field-free case is given by the dashed black line and for optical laser dressing by the dashed red, blue, and green lines.

is apparent in Fig. 3(b) that temporal control over the XRL is possible. The peak of the averaged SSG is shifted towards the peak of the optical dressing laser for each of the three cases. The modulation of the SSG results from the increase of the K-shell absorption cross section by optical laser dressing as seen in Fig. 2 (bottom), and gives rise to a modulation of the rate at which the upper-level population and thus the population inversion are built up. However, the optical laser does not affect processes that destroy the population inversion, namely, the decay rate of the upper level and the rate of valence ionization which also reduce the occupancy of the upper level. Therefore, optical laser dressing allows for the buildup of a larger population inversion than in the optical-field-free case.

IV. PROPAGATION IN A MEDIUM

Based on the analysis of the SSG in Sec. III, which describes x-ray lasing in the exponential gain regime, it seems feasible to control the XRL with a copropagating optical laser. For a macroscopic medium, the propagation of the optical laser, the FEL x rays, and the XRL x rays need to be investigated in detail. The ground-state population $N_G(z,t)$ at position z along the beam axis as a function of time t is determined by the rate equation [18]:

$$\frac{dN_G(z,t)}{dt} = -\frac{I_P(z,t)}{\omega_P} \left(\bar{\sigma}_X(I_L(z,t)) + \sigma_G\right) N_G(z,t), \tag{3}$$

which depends on the FEL x-ray intensity $I_P(z,t)$ and the weighted-average core-excitation cross section of the optical-laser-dressed atoms,

$$\bar{\sigma}_X(I_L) = \frac{\int_0^\infty \sigma_X(I_L,\omega)\,\frac{S_P(z,\omega)}{\omega}\,d\omega}{\int_0^\infty \frac{S_P(z,\omega)}{\omega}\,d\omega}. \quad (4)$$

The photoexcitation rate is the first term on the right-hand side of Eq. (3). It is expressed in terms of the weighted average (4) of $\sigma_X(I_L,\omega)$ with the spectral intensity $S_P(z,\omega) = \frac{c}{4\pi^2}|E_P(z,\omega)|^2$ of the FEL x-ray pulse—converted to the spectral flux by dividing by ω—that is defined with respect to the Fourier-transformed electric field of the FEL x rays $E_P(z,\omega)$ [18,34]. We specify the FEL photon flux by $\frac{I_P(z,t)}{\omega_P}$ and, in doing so, approximate the FEL x rays as monochromatic, which is justified by $\frac{\Delta\omega_P}{\omega_P} = 5\times10^{-4} \ll 1$. Nonetheless, the variation of the core-excitation cross section $\sigma_X(I_L,\omega)$ with respect to the frequencies ω in the pump pulse is accounted for using $\bar{\sigma}_X(I_L)$. Expression (4) accounts for the fact that different frequency components of the FEL x-ray pulse core-excite optical-laser-dressed atoms at varying rates due to the variation of the cross section $\sigma_X(I_L,\omega)$ around the FEL central frequency ω_P (Fig. 2). The second term on the right-hand side of Eq. (3) stands for the loss of ground-state population due to valence ionization by the FEL x rays which is determined by the cross section $\sigma_G = 23.8$ kb [35] where we neglect the influence of the optical laser dressing on σ_G which is minimal because photoelectrons are ejected with a large kinetic energy [22].

The FEL pump pulse is absorbed by the atoms in the medium in the course of the propagation as described by Eqs. (3), (5), (6), and (7). The temporal and spatial evolution of the FEL pump intensity [18] is given by

$$\frac{dI_P(z,t)}{dt} = -c\,n_\#\,I_P(z,t)\,[(\bar{\sigma}_X(I_L(z,t)) + \sigma_G)\,N_G(z,t) + \sigma_U\,N_U(z,t) + \sigma_L\,N_L(z,t)] - c\,\frac{dI_P(z,t)}{dz}, \quad (5)$$

where $n_\#$ is the atomic number density of the lasing medium. The three summands in the bracket on the right-hand side of Eq. (5) account for the absorption of the FEL x rays by atoms in the ground state and by atoms in the upper and lower levels with the occupancies $N_U(z,t)$ and $N_L(z,t)$ where the total absorption cross sections are $\sigma_U = 32.8$ kb for the upper and $\sigma_L = 24.2$ kb for the lower lasing level, respectively [35]. The last term on the bottom line of Eq. (5) represents the change of FEL pump intensity due to the traveling of the FEL pulse in the positive z direction with the speed of light in vacuum c.

In order to determine the impact of optical laser dressing on the XRL, we need to calculate its output intensity $I_X(z,t)$ for varying FEL pulse shapes. The occupancy of the upper lasing level $N_U(z,t)$ is found by considering all processes that build up or remove population in terms of the rate equation

$$\frac{dN_U(z,t)}{dt} = \frac{I_P(z,t)}{\omega_P}\,\bar{\sigma}_X(I_L(z,t))\,N_G(z,t) - \frac{I_X(z,t)}{\omega_X}\,g(z,t) - \left[\Gamma_A + A_{U\to L} + \frac{I_P(z,t)}{\omega_P}\,\sigma_U\right] N_U(z,t). \quad (6)$$

The first term on the right-hand side of the top line of Eq. (6) represents the rate at which the upper level is populated via photoexcitation by the FEL x rays. The second term on the right-hand side of Eq. (6) is the position z and time dependent SSG $g(z,t)$, defined in analogy to Eq. (1), multiplied by the flux of the XRL light which is treated as being monochromatic in good approximation because $\frac{\Delta\omega_X}{\omega_X} = 3\times10^{-4} \ll 1$. This term specifies the rate of XRL transitions between the lower and the upper levels where a positive (negative) SSG leads to a reduction (increase) of the upper-level occupancy. The first term on the bottom line of Eq. (6) accounts for Auger decay of the upper lasing level with the rate $\Gamma_A = 3.8\times10^{14}\ \mathrm{s}^{-1}$ [13]. The second term describes spontaneous emission that moves population from the upper to the lower lasing level, and the third term stands for valence ionization by the FEL x rays that destroy the atoms. As the XRL photon energy $\omega_X < \omega_P$, core excitation cannot be induced by the XRL light. Valence ionization by the XRL light is omitted from Eq. (6), as in Refs. [16,18], because the valence ionization cross section at ω_X is small and thus the FEL x rays will have excited or ionized the atoms before the XRL intensity has reached a magnitude that would make valence ionization by the XRL light competitive with valence ionization by FEL x rays.

The occupancy of the lower lasing level $N_L(z,t)$ is determined by the rate equation

$$\frac{dN_L(z,t)}{dt} = \frac{I_P(z,t)}{\omega_P}\,\sigma_{G,2p}\,N_G(z,t) + A_{U\to L}\,N_U(z,t) + \frac{I_X(z,t)}{\omega_X}\,g(z,t) - \frac{I_P(z,t)}{\omega_P}\,\sigma_L\,N_L(z,t). \quad (7)$$

In contrast to Eq. (6), the population of the lower XRL level in the top line on the right-hand side of Eq. (7) is obtained, by the first term, from the valence-ionization cross section of the $2p$ electrons of the ground-state atoms $\sigma_{G,2p} = 7.70$ kb [35,36] and, by the second term, from the transition rate from the upper to the lower level due to spontaneous emission. In the bottom line, the first term contains the SSG (1) and has the opposite sign as the corresponding term in Eq. (6); the second term accounts for the destruction of the atoms in the lower lasing level by valence ionization by the FEL x rays [18], where valence ionization by the XRL light is again not included.

The XRL intensity $I_X(z,t)$ is influenced by the occupancies of the upper and lower levels, which determine the SSG (1), in the course of the propagation in the medium. Specifically, light with the XRL transition frequency is attenuated for a negative SSG and it is amplified for a positive SSG as described by

$$\frac{dI_X(z,t)}{dt} = c\,n_\#\left[I_X(z,t)\,g(z,t) + \omega_X\,\frac{\Omega(z)}{4\pi}\,A_{U\to L}\,N_U(z,t)\right] - c\,\frac{dI_X(z,t)}{dz}. \quad (8)$$

The first term on the right-hand side of Eq. (8) describes stimulated emission and absorption of light from the XRL pulse via the SSG [Eq. (1)], whereas the second term represents the rate of spontaneous emission which initiates x-ray lasing in the forward direction because the XRL intensity is zero in the beginning. Only photons emitted into the solid angle

$$\Omega(z) = 2\pi\left(1 - \frac{L-z}{\sqrt{w_0^2 + (L-z)^2}}\right) \quad (9)$$

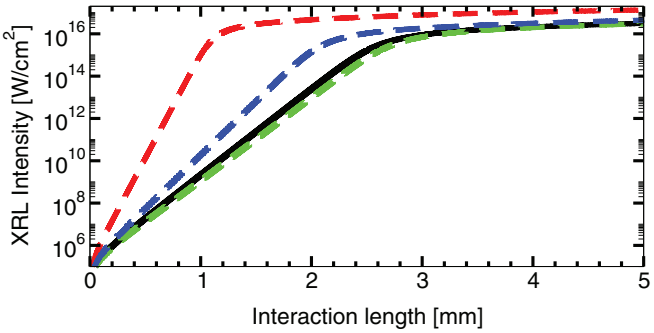

FIG. 4. (Color) Dependence of the XRL output intensity on the interaction length (or propagation distance) in a macroscopic medium. The XRL is pumped by the dashed black FEL pulse displayed in Fig. 3(a), which leads to the XRL output intensity that is given by the solid black line. The XRL output intensities with dressing by the optical laser pulses from Fig. 3(a) are shown as dashed lines of the same color here.

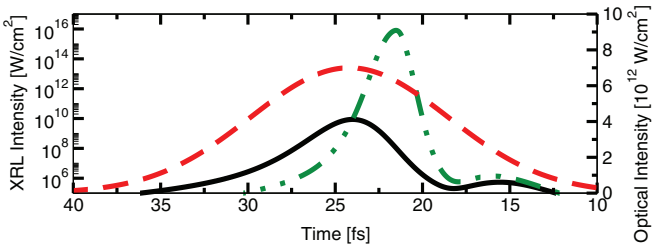

FIG. 5. (Color online) The temporal profile of the XRL pulses after saturation. The XRL is pumped with the dashed black FEL pulse from Fig. 3(a). The solid black line corresponds to the FEL-x-ray-only case and the dot-dashed green line displays the optical laser-dressed case by the dashed red optical laser pulse from Fig. 3(a), which is shown here as well.

contribute to x-ray lasing because only these photons stay completely within the XRL medium of length L and beam waist w_0 for the remainder of the propagation [16,18]. The bottom line of Eq. (8) stands for the propagation of the XRL light traveling in the positive z direction.

We use a fourth-order Runge-Kutta algorithm [1] to solve the linear system of first-order ordinary differential equations constituted by Eqs. (3), (6), and (7), transformed to a reference frame traveling with the speed of light. This gives the temporal evolution of the occupancy of the ground state $N_G(z,t)$ and the upper $N_U(z,t)$ and the lower $N_L(z,t)$ lasing levels for position z at time t. Equations (5) and (8) are solved through first-order forward stepping to find the pump $I_P(z,t)$ and XRL $I_X(z,t)$ intensities [1,18].

We apply Eqs. (3), (5), (6), (7), and (8) to our XRL scheme and calculate $I_X(z,t)$ depending on the interaction length (or propagation distance), which is the distance that the FEL, optical laser, and XRL pulses have propagated in a gas cell with $n_\# = 1 \times 10^{19}$ cm^{-3}. *Nota bene*, the z coordinate in $I_X(z,t)$ does not represent the propagation distance but describes the longitudinal spatial profile of the XRL pulses for an instant in time t. In Fig. 4, we display $I_X(z,t)$ of an XRL pumped by the FEL x rays only and with additional optical laser dressing for the three cases shown in Fig. 3(a). These are single-shot calculations of the XRL output intensity for the single-shot SSGs displayed in Fig. 3(b). Significant modulation of the XRL intensity is only provided by the dashed red optical laser pulses displayed in Fig. 3(a). The other optical laser pulses do not overlap with the rising flank of the FEL pump pulse and thus only slightly alter the XRL intensity with interaction length.

The temporal profiles of the XRL pulse after propagation through the medium for the FEL-x-ray only case and for optical laser dressing with the dashed red optical laser pulse are shown in Fig. 5. The small peak at the front of the XRL pulses is ascribed to emission processes from a small population inversion caused by the small peak in the FEL pulse found at approximately 15 fs in Fig. 3(a). The comparison of the solid black and dot-dashed green lines reveals that optical laser dressing leads to an increase by about six orders of magnitude of the XRL's peak intensity. Hence, the XRL's output intensity can be controlled via optical laser dressing. The FWHM duration of the XRL pulse from the FEL-x-ray-only case in Fig. 5 is compressed from 2.0 fs down to 0.7 fs if the dashed red optical laser pulse is used due to a faster buildup of population inversion in the latter case compared with the former case. Furthermore, Fig. 5 reveals that the XRL pulse is synchronized to the optical laser pulse with a time jitter of better than 5 fs. At peak FEL intensities reaching 4×10^{17} W/cm^2, the first few femtoseconds of the FEL pulse induce a complete population inversion, i.e., all neon atoms are either core excited afterwards or valence ionized, such that the remainder of the pulse passes through the gas without further interaction with core electrons. The energy efficiency of the XRL, i.e., the number of FEL photons that actually contribute to core excitation of the macroscopic medium, can be improved by reducing the FEL's peak intensity or shortening its pulses; however, reducing the FEL peak intensity leads to longer and less intense XRL pulses [18].

V. CONCLUSION

We propose an inner-shell XRL scheme that allows one to produce controlled, fully coherent, single-peak x-ray pulses with intensities above 1×10^{16} W/cm^2 which are synchronized to an optical laser pulse with femtosecond accuracy. In our scheme, optical-laser-controlled core excitation produces a state of population inversion; spontaneously emitted x rays which propagate along the beam axis of the FEL pump x rays are then amplified by stimulated emission leading to x-ray lasing.

Our XRL scheme can be modified in such a way that it works inversely to what has been discussed in this work by shifting the central frequency ω_P of the FEL x rays to the $1s \rightarrow 1s^{-1}3p$ resonance. Then, the optical laser dressing suppresses the K-shell absorption cross section by core electrons of neon as seen in Fig. 2 and x rays from the FEL are only absorbed efficiently when optical light is not present. This can be used to produce a short XRL pulse from a long FEL x-ray pulse by applying a long optical laser pulse with an interruption of a few femtoseconds.

Our proposed XRL goes beyond what can be realized at present-day x-ray FELs and will stimulate feasible and

attractive future x-ray science. Especially challenging for an experimental realization of our scheme is the achievement of 3×10^{13} FEL photons in a 0.4 eV bandwidth interval which is not currently possible, for example, at the soft x-ray instrument of LCLS for which estimates reveal that about 2×10^{10} photons are available under such conditions [37]. Our idea thus opens up perspectives for future two-color pump-probe experiments.

The optically controlled XRL offers a different way to measure the time jitter between FEL radiation and an optical laser that complements existing methods at present-day facilities [9]. Namely, choosing a length of the gas cell of 1.1 mm (Fig. 4) and placing a suitable filter [38] behind the gas cell that absorbs an intensity of up to 1×10^{11} W/cm^2, the output of the FEL-x-ray-only XRL can be entirely absorbed. Then, XRL output is only generated when the optical laser pulse overlaps with the front of the FEL pulse. This allows one to determine the overlap between x rays and the optical laser with femtosecond precision. Also the FEL x rays are damped down by many orders of magnitude by the propagation in the macroscopic medium and by the filter afterwards. Since the photon energies of the XRL and the FEL are comparable, the filter attenuates both beams by similar amounts. In order to distinguish between XRL light and FEL x rays, either a spectrometer is required to resolve the different photon energies or an inclined-beam experimental setup needs to ensure a spatial separation of both beams after propagation through the medium.

Multicolor x-ray lasing on several transitions, as predicted for a core-ionization-pumped XRL [16], is substantially suppressed by using core excitations because the chosen FEL photon energy of $\omega_{\mathrm{P}} = 868.2$ eV is far off resonant, e.g., with the $1s \rightarrow 1s^{-1}2p$ and $1s \rightarrow 1s^{-1}3p$ resonances in singly charged neon cations at transition energies of 848.66 and 885.8 eV, respectively [21]. If one is only interested in suppressing multicolor x-ray lasing, then the FEL x-ray energy may be tuned to the $1s \rightarrow 1s^{-1}3p$ resonance. Such a core-excitation-pumped XRL has the added benefit of a larger SSG [Eq. (1)] compared with a core-ionization-pumped XRL. This gives rise to a more rapid increase of the XRL output intensity with propagation distance in the macroscopic medium (Fig. 4), leading to a higher achievable saturation intensity of the XRL.

So far we have considered a constant transverse intensity profile of the optical laser and the FEL x rays. By choosing a transverse intensity profile for the optical laser pulse which is not constant [1], allows one to imprint such a profile onto the transverse intensity profile of the XRL pulse, i.e., transverse pulse shaping is facilitated.

ACKNOWLEDGMENTS

We would like to thank Stefano M. Cavaletto for fruitful discussions. C.B. was supported by the Chemical Sciences, Geosciences, and Biosciences Division of the Office of Basic Energy Sciences, Office of Science, U.S. Department of Energy, under Contract No. DE-AC02-06CH11357.

[1] P. W. Milonni and J. H. Eberly, *Laser Physics*, 2nd ed. (Wiley, Hoboken, NJ, 2010).

[2] J. J. Rocca, Rev. Sci. Instrum. **70**, 3799 (1999); S. Suckewer and P. Jaeglé, Laser Phys. Lett. **6**, 411 (2009).

[3] B. W. Adams, C. Buth, S. M. Cavaletto, J. Evers, Z. Harman, C. H. Keitel, A. Pálffy, A. Picón, R. Röhlsberger, Y. Rostovtsev, and K. Tamasaku, in *Physics in Quantum Electronics*, special issue of J. Mod. Opt. **60**, 2 (2013); R. Röhlsberger, H.-C. Wille, K. Schlage, and B. Sahoo, Nature (London) **482**, 199 (2012).

[4] A. Di Piazza, C. Müller, K. Z. Hatsagortsyan, and C. H. Keitel, Rev. Mod. Phys. **84**, 1177 (2012); S. Bernitt, G. V. Brown, J. K. Rudolph, R. Steinbrügge, A. Graf, M. Leutenegger, S. W. Epp, S. Eberle, K. Kubiček, V. Mäckel, M. C. Simon, E. Träbert, E. W. Magee, C. Beilmann, N. Hell, S. Schippers, A. Müller, S. M. Kahn, A. Surzhykov, Z. Harman, C. H. Keitel, J. Clementson, F. S. Porter, W. Schlotter, J. J. Turner, J. Ullrich, P. Beiersdorfer, and J. R. Crespo López-Urrutia, Nature (London) **492**, 225 (2012).

[5] F. Krausz and M. Ivanov, Rev. Mod. Phys. **81**, 163 (2009); S. M. Cavaletto, Z. Harman, C. Buth, and C. H. Keitel, Phys. Rev. A **88**, 063402 (2013); S. M. Cavaletto, Z. Harman, C. Ott, Christian Buth, T. Pfeifer, and C. H. Keitel (unpublished).

[6] J. M. J. Madey, J. Appl. Phys. **42**, 1906 (1971); E. L. Saldin, E. A. Schneidmiller, and M. V. Yurkov, *The Physics of Free Electron Lasers* (Springer, Berlin, 2000).

[7] J. Arthur *et al.*, Report No. SLAC-R-593, UC-414 (2002), http://www-ssrl.slac.stanford.edu/lcls/cdr; P. Emma *et al.*, Nat. Photonics **4**, 641 (2010).

[8] A. M. Kondratenko and E. L. Saldin, Dokl. Akad. Nauk SSSR **249**, 843 (1979) [Sov. Phys. Dokl. **24**, 986 (1979)]; R. Bonifacio, C. Pellegrini, and L. M. Narducci, Opt. Commun. **50**, 373 (1984).

[9] M. R. Bionta, H. T. Lemke, J. P. Cryan, J. M. Glownia, C. Bostedt, M. Cammarata, J.-C. Castagna, Y. Ding, D. M. Fritz, A. R. Fry, J. Krzywinski, M. Messerschmidt, S. Schorb, M. L. Swiggers, and R. N. Coffee, Opt. Express **19**, 21855 (2011); S. Schorb, T. Gorkhover, J. P. Cryan, J. M. Glownia, M. R. Bionta, R. N. Coffee, B. Erk, R. Boll, C. Schmidt, D. Rolles, A. Rudenko, A. Rouzee, M. Swiggers, S. Carron, J.-C. Castagna, J. D. Bozek, M. Messerschmidt, W. F. Schlotter, and C. Bostedt, Appl. Phys. Lett. **100**, 121107 (2012); M. Harmand, R. Coffee, M. R. Bionta, M. Chollet, D. French, D. Zhu, D. M. Fritz, H. T. Lemke, N. Medvedev, B. Ziaja, S. Toleikis, and M. Cammarata, Nat. Photonics **7**, 215 (2013).

[10] E. Allaria *et al.*, Nat. Photonics **6**, 699 (2012).

[11] J. Amann, W. Berg, V. Blank, F.-J. Decker, Y. Ding, P. Emma, Y. Feng, J. Frisch, D. Fritz, J. Hastings, Z. Huang, J. Krzywinski, R. Lindberg, H. Loos, A. Lutman, H.-D. Nuhn, D. Ratner, J. Rzepiela, D. Shu, Y. Shvyd'ko, S. Spampinati, S. Stoupin, S. Terentyev, E. Trakhtenberg, D. Walz, J. Welch, J. Wu, A. Zholents, and D. Zhu, Nat. Photonics **6**, 693 (2012).

[12] J. Als-Nielsen and D. McMorrow, *Elements of Modern X-ray Physics* (Wiley, New York, 2001).

[13] V. Schmidt, *Electron Spectrometry of Atoms Using Synchrotron Radiation* (Cambridge University Press, Cambridge, 1997).

[14] M. A. Duguay and P. M. Rentzepis, Appl. Phys. Lett. **10**, 350 (1967).

[15] K. Lan, E. Fill, and J. Meyer-ter-Vehn, Laser Part. Beams **22**, 261 (2004).
[16] N. Rohringer and R. London, Phys. Rev. A **80**, 013809 (2009); **82**, 049902(E) (2010); N. Rohringer, J. Phys.: Conf. Ser. **194**, 012012 (2009).
[17] D. R. Hartree, Math. Proc. Cambridge Philos. Soc. **24**, 89 (1928).
[18] G. Darvasi, master's thesis, Ruprecht-Karls-Universität Heidelberg, Heidelberg, Germany, 2011, Uniform Resource Name (URN): urn:nbn:de:bsz:16-opus-132045, HeiDOK - Der Heidelberger Dokumentenserver: http://www.ub.uni-heidelberg.de/archiv/13204.
[19] H. C. Kapteyn, Ph.D. thesis, University of California, Berkeley, California, USA, 1989, http://jila.colorado.edu/~kapteyn/Research/Thesis%20formatted.pdf; Appl. Opt. **31**, 4931 (1992).
[20] N. Rohringer, D. Ryan, R. A. London, M. Purvis, F. Albert, J. Dunn, J. D. Bozek, C. Bostedt, A. Graf, R. Hill, S. P. Hau-Riege, and J. J. Rocca, Nature (London) **481**, 488 (2012).
[21] M. Oura, Plasma Sci. Technol. **12**, 353 (2010).
[22] C. Buth, R. Santra, and L. Young, Phys. Rev. Lett. **98**, 253001 (2007).
[23] R. Santra, C. Buth, E. R. Peterson, R. W. Dunford, E. P. Kanter, B. Krässig, S. H. Southworth, and L. Young, J. Phys.: Conf. Ser. **88**, 012052 (2007).
[24] H. R. Varma, L. Pan, D. R. Beck, and R. Santra, Phys. Rev. A **78**, 065401 (2008); R. Santra, R. W. Dunford, E. P. Kanter, B. Krässig, S. H. Southworth, and L. Young, in *Advances in Atomic, Molecular, and Optical Physics*, Vol. 56, edited by E. Arimondo, P. R. Berman, and C. C. Lin (Academic Press, Amsterdam, 2008), pp. 219–259; C. Buth, R. Santra, and L. Young, Rev. Mex. Fís. S **56**, 59 (2010); L. Young, C. Buth, R. W. Dunford, P. J. Ho, E. P. Kanter, B. Krässig, E. R. Peterson, N. Rohringer, R. Santra, and S. H. Southworth, *ibid.* **56**, 11 (2010); T. E. Glover, M. P. Hertlein, S. H. Southworth, T. K. Allison, J. van Tilborg, E. P. Kanter, B. Krässig, H. R. Varma, B. Rude, R. Santra, A. Belkacem, and L. Young, Nat. Phys. **6**, 69 (2010).
[25] C. Buth and R. Santra, Phys. Rev. A **78**, 043409 (2008); FELLA: The free electron laser atomic, molecular, and optical physics program package, version 1.3.0 (Argonne National Laboratory, Argonne, Illinois, USA, 2008), with contributions by Mark Baertschy, Kevin Christ, Chris H. Greene, Hans-Dieter Meyer, and Thomas Sommerfeld.
[26] C. Buth and R. Santra, Phys. Rev. A **75**, 033412 (2007).
[27] M. B. Gaarde, C. Buth, J. L. Tate, and K. J. Schafer, Phys. Rev. A **83**, 013419 (2011).
[28] The optical-laser-intensity-dependent x-ray absorption cross section of core electrons of neon is plotted in Fig. 2 of Ref. [23] on the $1s \rightarrow 1s^{-1}3p$ resonance.
[29] M. Dörr, O. Latinne, and C. J. Joachain, Phys. Rev. A **52**, 4289 (1995).
[30] H. Ågren, J. Nordgren, L. Selander, C. Nordling, and K. Siegbahn, J. Electron Spectrosc. Relat. Phenom. **14**, 27 (1978).
[31] A. De Fanis, N. Saito, H. Yoshida, Y. Senba, Y. Tamenori, H. Ohashi, H. Tanaka, and K. Ueda, Phys. Rev. Lett. **89**, 243001 (2002).
[32] T. Pfeifer, Y. Jiang, S. Düsterer, R. Moshammer, and J. Ullrich, Opt. Lett. **35**, 3441 (2010); Y. H. Jiang, T. Pfeifer, A. Rudenko, O. Herrwerth, L. Foucar, M. Kurka, K. U. Kühnel, M. Lezius, M. F. Kling, X. Liu, K. Ueda, S. Düsterer, R. Treusch, C. D. Schröter, R. Moshammer, and J. Ullrich, Phys. Rev. A **82**, 041403(R) (2010); S. M. Cavaletto, C. Buth, Z. Harman, E. P. Kanter, S. H. Southworth, L. Young, and C. H. Keitel, *ibid.* **86**, 033402 (2012).
[33] The beam waist of the optical laser is chosen sufficiently large to ensure a confocal parameter [1,34] that is bigger than the length L of the gas cell.
[34] J.-C. Diels and W. Rudolph, *Ultrashort Laser Pulse Phenomena*, 2nd ed., Optics and Photonics Series (Academic Press, Amsterdam, 2006).
[35] R. D. Cowan, *The Theory of Atomic Structure and Spectra*, Los Alamos Series in Basic and Applied Sciences (University of California Press, Berkeley, California, USA, 1981); Los Alamos National Laboratory, Atomic Physics Codes, http://aphysics2.lanl.gov/tempweb/lanl.
[36] In specifying the first term on the right-hand side of Eq. (7) involving $\sigma_{G,2p}$, we do not distinguish between valence-ionized atoms and valence-excited atoms as lower lasing level.
[37] W. F. Schlotter *et al.*, Rev. Sci. Instrum. **83**, 043107 (2012).
[38] B. L. Henke, E. M. Gullikson, and J. C. Davis, At. Data Nucl. Data Tables **54**, 181 (1993); The Center for X-Ray Optics, Lawrence Berkeley National Laboratory, Berkeley, California, USA, 2010, http://henke.lbl.gov/optical_constants.